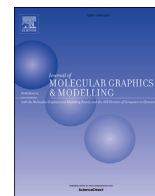




Since January 2020 Elsevier has created a COVID-19 resource centre with free information in English and Mandarin on the novel coronavirus COVID-19. The COVID-19 resource centre is hosted on Elsevier Connect, the company's public news and information website.

Elsevier hereby grants permission to make all its COVID-19-related research that is available on the COVID-19 resource centre - including this research content - immediately available in PubMed Central and other publicly funded repositories, such as the WHO COVID database with rights for unrestricted research re-use and analyses in any form or by any means with acknowledgement of the original source. These permissions are granted for free by Elsevier for as long as the COVID-19 resource centre remains active.



# Prioritizing potential ACE2 inhibitors in the COVID-19 pandemic: Insights from a molecular mechanics-assisted structure-based virtual screening experiment

Kerem Terali <sup>a, b, \*</sup>, Buket Baddal <sup>c, d</sup>, Hayrettin Ozan Gülcan <sup>e</sup>

<sup>a</sup> Department of Medical Biochemistry, Near East University, Nicosia, 99138, Cyprus

<sup>b</sup> Bioinformatics & Computational Biology Research Group, DESAM Institute, Near East University, Nicosia, 99138, Cyprus

<sup>c</sup> Department of Medical Microbiology and Clinical Microbiology, Near East University, Nicosia, 99138, Cyprus

<sup>d</sup> Microbial Pathogenesis Research Group, DESAM Institute, Near East University, Nicosia, 99138, Cyprus

<sup>e</sup> Department of Pharmaceutical Chemistry, Eastern Mediterranean University, Famagusta, 99628, Cyprus

## ARTICLE INFO

### Article history:

Received 20 May 2020

Received in revised form

23 June 2020

Accepted 12 July 2020

Available online 23 July 2020

### Keywords:

SARS-CoV-2

COVID-19

ACE2

Drug repositioning

Entry inhibitor

## ABSTRACT

Angiotensin-converting enzyme 2 (ACE2) is a membrane-bound zinc metallopeptidase that generates the vasodilatory peptide angiotensin 1–7 and thus performs a protective role in heart disease. It is considered an important therapeutic target in controlling the COVID-19 outbreak, since SARS-CoV-2 enters permissive cells via an ACE2-mediated mechanism. The present *in silico* study attempted to repurpose existing drugs for use as prospective viral-entry inhibitors targeting human ACE2. Initially, a clinically approved drug library of 7,173 ligands was screened against the receptor using molecular docking, followed by energy minimization and rescoring of docked ligands. Finally, potential binders were inspected to ensure molecules with different scaffolds were engaged in favorable contacts with both the metal cofactor and the critical residues lining the receptor's active site. The results of the calculations suggest that lividomycin, burixafor, quisinostat, fluprofylline, pemetrexed, spirofylline, edotecarin, and diniprofylline emerge as promising repositionable drug candidates for stabilizing the closed (substrate/inhibitor-bound) conformation of ACE2, thereby shifting the relative positions of the receptor's critical exterior residues recognized by SARS-CoV-2. This study is among the rare ones in the relevant scientific literature to search for potential ACE2 inhibitors. In practical terms, the drugs, unmodified as they are, may be introduced into the therapeutic armamentarium of the ongoing fight against COVID-19 now, or their scaffolds may serve as rich skeletons for designing novel ACE2 inhibitors in the near future.

© 2020 Elsevier Inc. All rights reserved.

## 1. Introduction

A previously unknown coronavirus (CoV) has crossed the species barrier and emerged as the novel severe acute respiratory syndrome coronavirus 2, SARS-CoV-2, in Wuhan, Hubei province of China in December 2019. SARS-CoV-2 has been identified as the causative agent of atypical pneumonia, now termed coronavirus disease 19 (COVID-19). Despite the containment efforts public health authorities in China initiated, SARS-CoV-2 has quickly spread across the globe currently affecting over 210 countries and

territories. The World Health Organization (WHO) declared SARS-CoV-2 as a pandemic on 11 March 2020 [1]. As of 17 May 2020, COVID-19 has affected 4,525,497 people worldwide with 307,395 deaths reported [2]. SARS-CoV-2 belongs to the same family and genus of highly pathogenic emerging viruses, betacoronaviruses, that primarily cause enzootic infections in birds and mammals and have demonstrated strong lethality in humans such as the well-known severe acute respiratory syndrome coronavirus (SARS-CoV) and Middle East respiratory syndrome coronavirus (MERS-CoV), which have killed hundreds of people over the past 17 years [3]. Despite being implicated as a major public health concern, to date, no effective therapeutics have been approved against SARS-CoV-2, with a number of treatment options (remdesivir; lopinavir with ritonavir; lopinavir with ritonavir plus interferon beta-1a; and

\* Corresponding author. Department of Medical Biochemistry, Near East University, Near East Boulevard, Nicosia, 99138, Cyprus.

E-mail address: [kerem.terali@neu.edu.tr](mailto:kerem.terali@neu.edu.tr) (K. Terali).

chloroquine or hydroxychloroquine) currently being under study [4]. Therefore, there is an urgent need for the development of effective treatment strategies for the control of the COVID-19 pandemic.

CoVs are non-segmented positive sense RNA viruses that are known to have four structural proteins, including envelope (E), membrane (M), nucleocapsid (N), and spike (S) proteins [5]. Among them, S glycoprotein plays the most important roles in viral attachment, fusion and entry and is the primary determinant of CoV tropism [6]. CoV entry into host cells is mediated by the transmembrane S glycoprotein that forms homotrimers protruding from the viral surface [7], and gives CoVs a crown-like appearance by forming spikes on their surface. S protein binds to a membrane receptor on the host cells, angiotensin-converting enzyme 2 (ACE2; EC 3.4.17.23) mediating the viral and cellular membrane fusion, which represents the critical initial stage of the infection. SARS-CoV-2 exploits human ACE2 for host cell entry [8,9], although CD147/S protein-mediated route of invasion has also recently been reported [10]. SARS-CoV-2 S protein comprises two functional subunits responsible for binding to the host cell receptor (S1 subunit) and fusion of the viral and cellular membranes (S2 subunit). Viral entry depends on binding of the S1 subunit to ACE2 through the receptor-binding domain (RBD) in the S1 subunit, facilitating viral attachment to the surface of target cells [11]. Additionally, entry requires S protein priming by cellular serine protease TMPRSS2, which entails S protein cleavage at the S1/S2 and the S2' site and allows fusion of viral and cellular membranes, a process driven by the S2 subunit [12]. Strikingly, SARS-CoV-2 has been shown to harbor a furin cleavage site at the S1/S2 boundary which is processed during biosynthesis, and which represents a novel feature setting SARS-CoV-2 S protein apart from SARS-CoV S protein that possesses a monobasic S1/S2 cleavage site processed upon entry into target cells [13].

ACE2, exploited by CoVs for viral entry, is a type I membrane protein expressed in lungs, kidneys, intestine, and heart [14–16]. Full-length ACE2 consists of an N-terminal peptidase domain (PD) and a C-terminal collectrin-like domain (CLD) that ends with a single transmembrane helix and a ~40-residue intracellular segment [14,17]. Structural information on ACE2 is limited to the zinc ( $Zn^{2+}$ )-dependent PD domain as its single transmembrane (TM) helix makes it challenging to determine the structure of the full-length protein. In a physiological context, ACE2, as part of the renin–angiotensin system (RAS), catalyzes the cleavage of angiotensin II to angiotensin 1–7, the latter being a potent vasodilator with protective properties for the cardiovascular system [18]. In order to facilitate countermeasure developments, a 3.5 Å-resolution cryo-electron microscopy structure of the SARS-CoV-2 S trimer in prefusion conformation has been recently determined. This analysis revealed that the predominant state of the trimer has one of the three RBDs rotated up in a receptor-accessible conformation, and also provided biophysical and structural evidence that the SARS-CoV-2 S protein ectodomain binds to the PD of ACE2 with an affinity of ~15 nM, which is ~10- to 20-fold higher than the affinity with which SARS-CoV S binds to ACE2 [19]. Further studies on the molecular basis of viral recognition using full-length ACE2 revealed that the SARS-CoV-2 RBD is recognized by the extracellular PD of ACE2 mainly through polar residues and that two S protein trimers can simultaneously bind to an ACE2 homodimer [20]. The X-ray crystallographic data on the complex structure of the SARS-CoV-2 RBD bound with ACE2 fully corroborated other evidence describing the residues in the SARS-CoV-2 RBD that are critical for ACE2 binding, the majority of which are highly conserved or share similar side chain properties with those in the SARS-CoV RBD [21].

Despite the COVID-19 research being largely focused on vaccines [22] and the virus's non-structural proteins such as main protease

( $M^{pro}$ ) and RNA-dependent RNA polymerase (RdRp) [23], we believe that ACE2 represents a significant target for investigating new SARS-CoV-2 infection prevention strategies. The very first crystal structures of the free and inhibitor-bound forms of ACE2 (at 2.2 Å and 3.0 Å resolutions, respectively) were solved back in 2004 [24]. A comparison of these structures illustrates a large, hinge-like motion of the two constituent parts (subdomains) of the PD of ACE2, by which the enzyme alternates between an 'open' conformation and a 'closed' conformation. The marked conformational change that accompanies inhibitor binding also heralds a shift in position of the aforementioned polar residues involved in recognizing the SARS-CoV-2 S protein. Indeed, using structure-based virtual screening (SBVS) of a chemical library of ~140,000 diverse compounds (synthetics), Huentelman et al. [25] discovered a novel ACE2 inhibitor (or, to be more accurate, a small-molecule lead compound), which also proved effective in blocking the SARS-CoV S protein-mediated cell fusion. The findings of this series of studies add experimental evidence to our belief. Drug repositioning (also called drug repurposing) describes the process of creating novel clinical opportunities for known, approved drugs. When compared to *de novo* drug discovery, drug repositioning not only shortens the time of chemical-structural optimization, but also reduces the cost of toxicological testing. This coherent therapeutic strategy has previously been used to develop effective treatments for other coronavirus infections, including MERS-CoV [26]. Here, using a molecular mechanics (MM)-assisted SBVS method, we search for 'new-old' drugs that potentially bind to and stabilize the closed conformation of ACE2.

## 2. Materials and methods

### 2.1. Protein preparation and chemical library selection

The atomic coordinates of recombinant human ACE2 in complex with the potent dipeptide-mimetic inhibitor MLN-4760 (PDB ID: 1R4L; resolution: 3.0 Å; *R*-value, free: 0.337; *R*-value, work: 0.253) [24] were retrieved from the RCSB Protein Data Bank [27] (available at <https://www.rcsb.org/>) and provided as input to the AddH utility of UCSF Chimera, Version 1.11.2 [28] for receptor preparation purposes. The RPBS Web portal's approved drugs collection Drugs-lib previously developed in-house [29] (available at <https://bioserv.rpbs.univ-paris-diderot.fr/>) was chosen by rational selection, based on the urgent need for repositioning existing medicines to prevent or treat COVID-19 in a safe, rapid and convenient manner.

### 2.2. Structure-based virtual screening

In order to identify the clinically approved drugs that are accommodated well in the active-site cleft of ACE2, the entire set of ligands deposited in Drugs-lib was virtually screened against the receptor (in its closed conformation) using an AutoDock Vina-based molecular docking approach adopted by the MTiOpenScreen Web service [30] (available at <https://mobyli.rpbs.univ-paris-diderot.fr/cgi-bin/portal.py#forms::MTiOpenScreen>). The conformational search space was defined as a cubic box centered at the center of mass of the co-crystallized inhibitor ( $x = 41.399$ ;  $y = 5.851$ ;  $z = 28.082$ ), with an edge length of 20 Å. All docking simulations were run with default settings, generating a maximum of 10 binding modes at an exhaustiveness level of 8.

### 2.3. Molecular mechanic optimization

In order to provide a more realistic description of the predicted protein–ligand complexes, successfully docked ligands were refined and subsequently rescored using the AMMOS2 Web service

[31] (available at <http://drugmod.rpbs.univ-paris-diderot.fr/ammosHome.php>) in a setting where the ligand and ACE2 side-chain atoms within 4 Å of the ligand were rendered flexible. During the sp4 AMMP force field-driven automatic energy minimization procedure, the catalytic active-site  $Zn^{2+}$  ion and structural (crystallographic) water molecules were also considered. Energy-minimized protein–ligand complexes, as prepared by the PLIP software [32] in the PDB format, were directly visualized in the PyMOL Molecular Graphics System, Version 1.8 (Schrödinger LLC, Portland, OR, USA), and favorable non-covalent interactions between ACE2 and selected drugs were analyzed using Discovery Studio Visualizer, Version 16.1.0 (Dassault Systèmes BIOVIA Corp., San Diego, CA, USA).

### 3. Results and discussion

The N-terminal PD of ACE2 (amino acid residues 19–615) has two distinct lobes or subdomains, which are connected by a hinge region and harbor the substrate/inhibitor-binding site in between [24]. When the larger subdomains (residues 103–289, 398–416, and 431–615) of the free (PDB ID: 1R42) and inhibitor-bound (PDB ID: 1R4L) ACE2 PDs are structurally aligned relative to the entire protein chain ( $C_{\alpha}$ -atom r.m.s. deviation = 0.520 Å), one can readily observe the large-scale atomic motion switching ACE2 from an open conformation to a closed conformation upon ligand binding (Fig. 1, left panel). The 13 polar residues (Gln<sup>24</sup>, Asp<sup>30</sup>, Glu<sup>35</sup>, Glu<sup>37</sup>, Asp<sup>38</sup>, Tyr<sup>41</sup>, Gln<sup>42</sup>, Tyr<sup>83</sup>, Gln<sup>325</sup>, Glu<sup>329</sup>, Asn<sup>330</sup>, Lys<sup>353</sup>, Arg<sup>393</sup>) that are involved in establishing hydrogen bonds and/or salt bridges with the SARS-CoV-2 RBD are mostly confined to the N-terminal helix of the smaller subdomain of the ACE2 PD [21]. When an inhibitor, such as the histidine-leucine mimetic MLN-4760, binds at the active site of the ACE2 PD, the SARS-CoV-2 RBD-interacting polar residues undergo relative spatial displacement, as measured by the distance between the  $C_{\alpha}$  atoms of the residues, that ranges from 1.7 to 12.0 Å (mean = 6.9 Å) (Fig. 1, right panel). Therefore, the substantial conformational rearrangements in the ACE2 PD that occur during the closure of the active-site cleft to achieve a

catalytic-competent geometry are reasonably likely to impede viral attachment to the surface of permissive cells.

MLN-4760 was tested on subjects with ulcerative colitis (which is interrelated with ACE2 overexpression) for safety, tolerability, and pilot therapeutic activity in a phase Ib/IIa clinical trial between 2009 and 2011, but the development of this investigational drug was abandoned by Ore Pharmaceuticals, Inc. due to concerns over toxicity (available at <https://clinicaltrials.gov/ct2/show/NCT01039597>). In an attempt to identify clinically approved drugs that can act as entry inhibitors in the early stages of SARS-CoV-2 infection by blocking viral fusion to ACE2-expressing cells, we employed an MM-aided SBVS method. Drugs-lib, which contains 7,173 stereoisomers corresponding to 4,574 single-isomer drugs, is a unique resource compiled from four popular compound databases – namely, the “drug” subsets of the ChEMBL and DrugCentral databases and the “approved” subsets of the DrugBank and SuperDRUG2 databases. Drugs-lib represents an ideal choice for our experiment not only because it is a comprehensive library of repurposing-friendly drugs, but also because it entirely consists of already protonated three-dimensional structures. AutoDock Vina generated 4,494 binding poses (which correspond to the three best poses of the 1,500 top-scoring ligands with a docking score range from –13.2 to –9.6 kcal/mol) in the closed active-site cleft of the target, all of which were subsequently submitted to the AMMOS2 energy minimization pipeline for optimization purposes. The top 3% of the rescored ligands were examined thoroughly to determine the network of interatomic contacts that stabilize the position of the drug in the active-site cleft of ACE2. This cut-off was selected on the basis of the previously described ability of AMMOS to enrich top 3–5% of an entire compound collection in known bioactive molecules as compared to decoys and unknown binders [33]. We validated our research methodology by redocking and refining MLN-4760. The co-crystal pose of the inhibitor was reproduced well, with a heavy-atom r.m.s. deviation of 0.842 Å (Fig. 2, left panel). It is also worth mentioning that no known potent angiotensin-converting enzyme (ACE; EC 3.4.15.1) inhibitors were found in the entire list of 4,494 docked ‘hits’, except for moexiprilat and

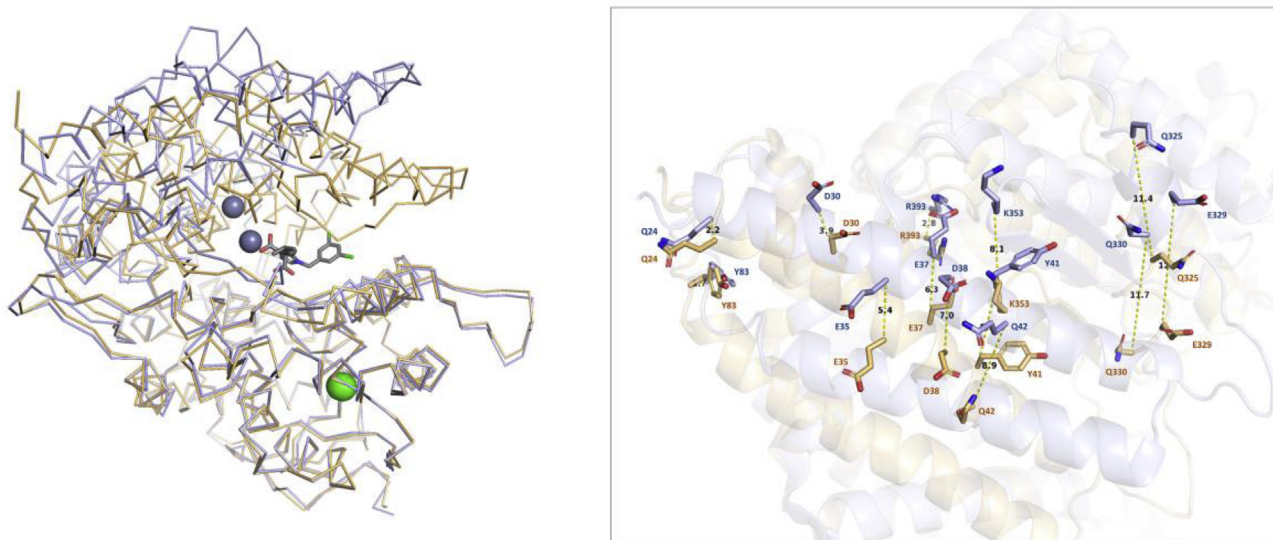


**Fig. 1.** **Left:**  $C_{\alpha}$ -atom wire representations of the inhibitor-free (in light blue; PDB ID:1R42) and inhibitor-bound (in light orange; PDB ID: 1R4L) states of human ACE2 aligned to each other based on their large subdomains (residues 103–289, 398–416, and 431–615). The catalytic  $Zn^{2+}$  ions are shown as blue-gray spheres, and the structural  $Cl^{-}$  ions are shown as lime green spheres. MLN-4760 is shown as silver sticks. The image was rendered using the PyMOL Molecular Graphics System, Version 1.8 (Schrödinger LLC, Portland, OR, USA). **Right:** Spatial displacement between the SARS-CoV-2 S protein-interacting residues of native ACE2 (in light blue) and those of inhibitor-bound ACE2 (in light orange). Distances between the  $C_{\alpha}$  atoms of the equivalent residues are shown as yellow dashed lines and measured in Å. The image was rendered using the PyMOL Molecular Graphics System, Version 1.8 (Schrödinger LLC, Portland, OR, USA). (For interpretation of the references to color in this figure legend, the reader is referred to the Web version of this article.)

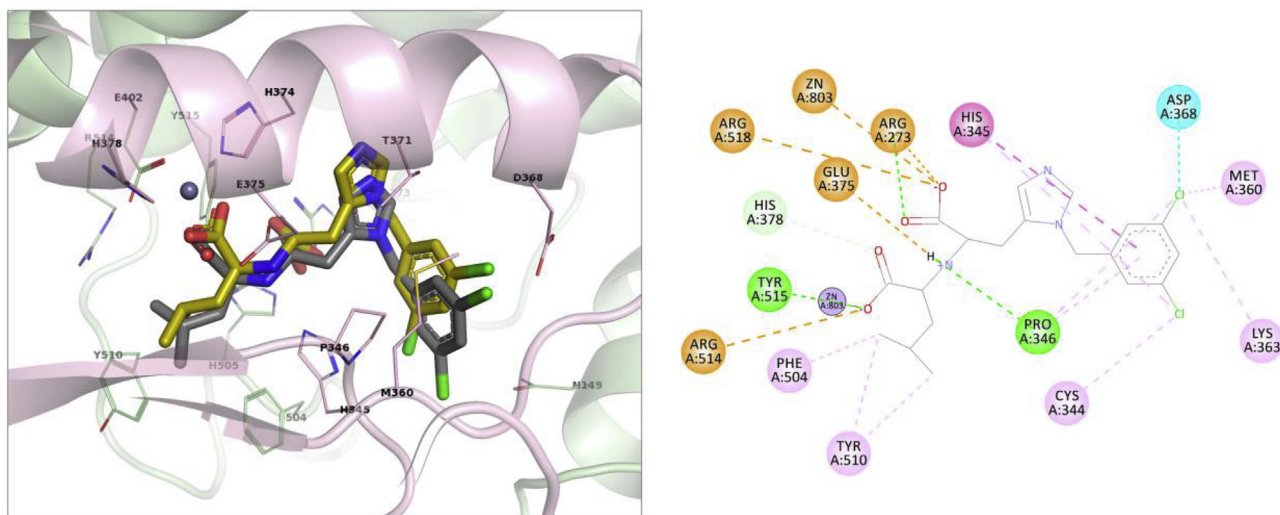


**Fig. 2.** *Left:* Close-up view of minimized MLN-4760 (in gold) superposed on the crystallographically determined ACE2–MLN-4760 complex (PDB ID: 1R4L). Side chains of residues within 4 Å of the co-crystallized inhibitor (in silver) are shown as lines. The  $Zn^{2+}$  ion is shown as a blue-gray sphere. The large subdomain is colored pale green, and the small subdomain is colored light pink. The image was rendered using the PyMOL Molecular Graphics System, Version 1.8 (Schrödinger LLC, Portland, OR, USA). *Right:* Two-dimensional view of favorable interactions anchoring the co-crystallized inhibitor in the active-site cleft of human ACE2 (PDB ID: 1R4L). Ionic interactions (salt bridges) and attractive charge interactions are shown as orange dashed lines. Conventional hydrogen bonds are shown as lime green dashed lines. Weak hydrogen bonds are shown as light turquoise dashed lines. Halogen bonds are shown as cyan dashed lines.  $\pi$ – $\pi$  interactions are shown as magenta dashed lines.  $\pi$ –alkyl and alkyl–alkyl interactions are shown as pink dashed lines. The image was rendered using Discovery Studio Visualizer, Version 16.1.0 (Dassault Systèmes BIOVIA Corp., San Diego, CA, USA). (For interpretation of the references to color in this figure legend, the reader is referred to the Web version of this article.)

quinaprilat. It has been shown that captopril, enalaprilat, lisinopril, cilazaprilat, indolaprilat, perindoprilat, quinaprilat and spiraprilat, rentiapril, zofenapril, ceranopril, and fosinoprilat fail to inhibit the peptidase activity of ACE2 at doses that affect ACE function [34,35]. The structural differences between the active-site clefts of these fairly homologous (identity = 42%; similarity = 60%) peptidases likely stem from the fact that the side chains of Arg<sup>273</sup>, Thr<sup>347</sup>, and Tyr<sup>510</sup> in ACE2 are relatively large compared to those of the corresponding residues in ACE [24]. In agreement with the above experimental observations, the computed interaction energies (in kcal/mol) of the refined (energy-minimized) ACE2–moexiprilat and ACE2–quinaprilat complexes have a positive sign. This not only confirms that ACE inhibitor (‘-pril’ or ‘-prilat’) binding to ACE2 is unfavorable, but also attests to the validity of our MM-assisted SBVS data.

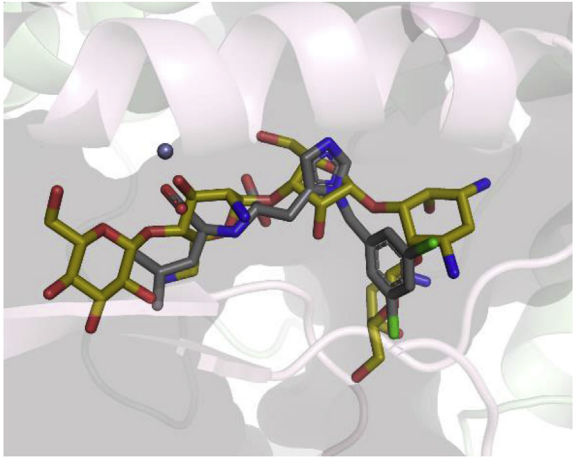
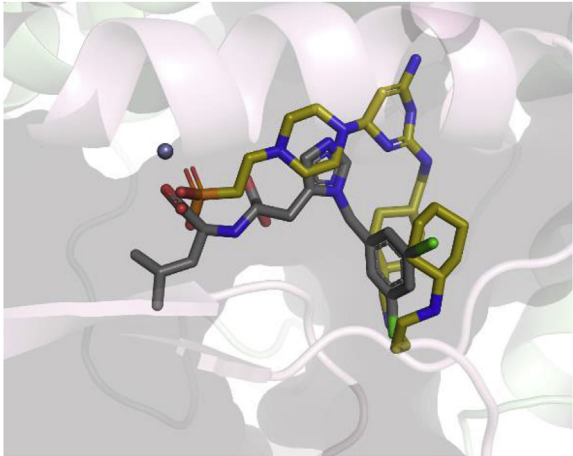
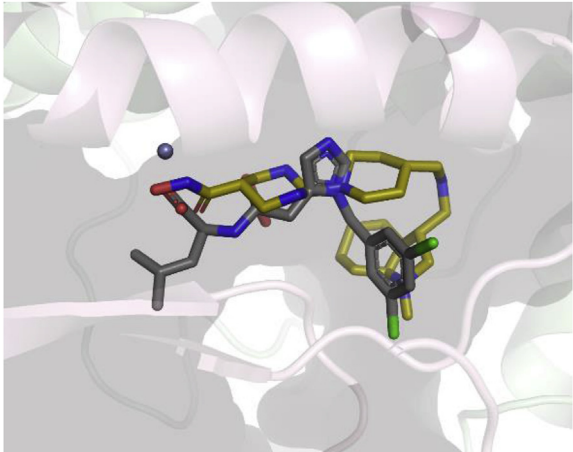
It is well established that metal ions, and in particular bivalent metal ions (e.g.  $Fe^{2+}$ ,  $Zn^{2+}$ , and  $Mg^{2+}$ ), are used by a striking number of enzymes (often referred to as metalloenzymes) for catalytic purposes. For example, statistics based on a total of 141,471 PDB structures (as of 18 September 2019) show that 22.2% of all metal-bound hydrolases (EC 3.-.-.-) are zinc-dependent [36] (available at <http://metalweb.cerm.unifi.it/>). Many FDA-approved drugs that target zinc-dependent metalloenzymes are known to be coordinated to the catalytic active-site  $Zn^{2+}$  ion through a zinc-binding group (ZBG). Common ZBGs include carboxylate-, sulfonamide-, hydroxamate- and phosphonate/phosphate-based functionalities, among others [37]. In the native structure of ACE2, the  $Zn^{2+}$  ion cofactor is coordinated by His<sup>374</sup>, His<sup>378</sup>, Glu<sup>402</sup>, and a water molecule to complete the tetrahedral geometry about the metal center. These residues compose the signature motif HEXXH + E (where X is any residue) that is conserved in the gluzincin family (clan MA) of zinc-dependent metalloproteases exemplified by thermolysin. As in the case of thermolysin, the water molecule is polarized by  $Zn^{2+}$  and stabilized by hydrogen-bonding interactions with a conserved glutamate residue (Glu<sup>375</sup>) in the second coordination sphere of the metal ion. Three key

active-site residues that play important roles in catalysis are Arg<sup>273</sup> (which is critical for substrate recognition), Glu<sup>375</sup> (which functions as a general base, and activates the zinc-bound water nucleophile), and His<sup>345</sup> (which functions as a hydrogen bond donor/acceptor, and stabilizes the tetrahedral intermediate). Another active-site residue of note, which is involved in catalysis, is His<sup>505</sup>. It does not, however, appear to be a transition state-stabilizing residue, as demonstrated in site-directed mutagenesis experiments [38]. Being a potent and selective ACE2 inhibitor ( $IC_{50} < 1$  nM), MLN-4760 forms rather strong directed interactions (e.g. coordinate covalent bonds, ionic interactions, and hydrogen bonds) with the atoms that constitute the receptor’s active site (Fig. 2, right panel). Accordingly, negative charges present on the inhibitor’s two carboxylate groups establish ionic interactions with positive charges present on the side chains of Arg<sup>514</sup>, Arg<sup>518</sup>, and Arg<sup>273</sup>. In addition, one of the carboxylate groups is also coordinated to the catalytic  $Zn^{2+}$  ion. Hydrogen-bonding interactions occur between the main chain of Pro<sup>346</sup> and the secondary amine group of the inhibitor as well as between the phenolic side chain of Tyr<sup>515</sup> and the zinc-bound carboxylate group of the inhibitor. The imidazole side chain of His<sup>345</sup> is able to make a  $\pi$ – $\pi$  interaction with the aromatic ring of the inhibitor. The position of MLN-4760 in the active-site cleft of ACE2 is further stabilized by halogen-bonding,  $\pi$ –alkyl and alkyl–alkyl interactions.

On the basis of the aforementioned features of the active-site cleft of ACE2, our analyses yielded eight promising repositionable drug candidates with the potential to interact with multiple residues from both the large and the small subdomains of the ACE2 PD (Table 1). It is important to note here that the small-molecule interactants (lividomycin, burixafor, quisinostat, fluprofylline, pemetrexed, spirofylline, edotecarin, and diniprofylline) belong to distinct pharmacological groups, except for fluprofylline, spirofylline, and diniprofylline that can be grouped into xanthine derivatives. To the best of our knowledge, these eight drugs have not been repurposed for use as anti-COVID-19 agents before. Equally importantly, no known ACE2 active-site binders have previously

**Table 1**

Promising repositionable drug candidates identified in the current MM-assisted SBVS study. Binding energies represent minimized protein–ligand interaction energies computed by AMMOS2. Each image shows the relative position, orientation, and conformation of the refined ligand (in gold) with respect to MLN-4760 (in silver) in the active-site cleft of human ACE2 (PDB ID: 1R4L). Hydrogen atoms are not shown for clarity. The images were rendered using the PyMOL Molecular Graphics System, Version 1.8 (Schrödinger LLC, Portland, OR, USA).

Drug	Binding energy (in kcal/mol)	Binding mode	Potential indications
<b>Lividomycin</b> , a second-line aminoglycoside antibiotic	−2,145.79		<i>Mycobacterium tuberculosis</i> , <i>Pseudomonas aeruginosa</i> and urinary tract infections; HIV infection(?)
<b>Burixafor</b> , a potent and selective CXCR4 antagonist	−2,108.82		Stem cell mobilization; hematological cancers; ischemic heart disease; HIV infection(?)
<b>Quisinostat</b> , a pan-histone deacetylase inhibitor with marked potency toward HDAC1	−1,998.77		Hematological cancers; non-small cell lung cancer; ovarian cancer; cardiac and pulmonary fibrosis(?)

(continued on next page)

Table 1 (continued)

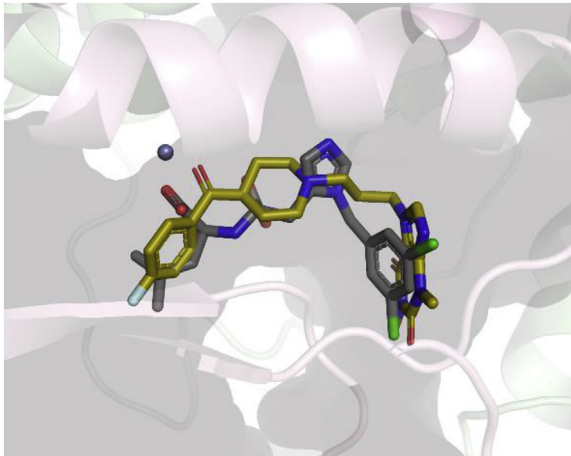
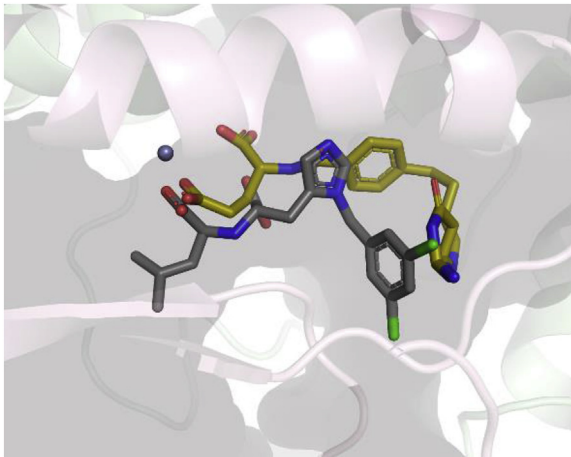
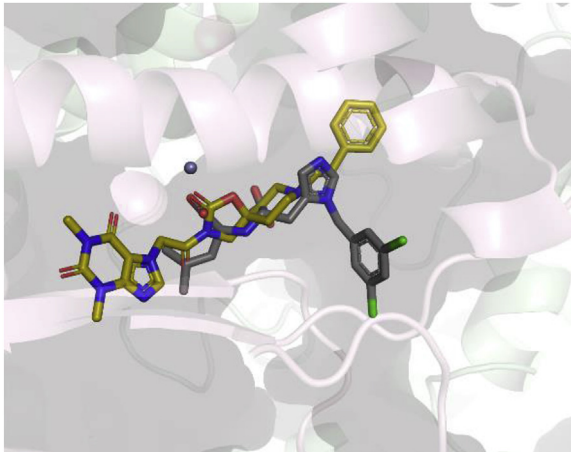
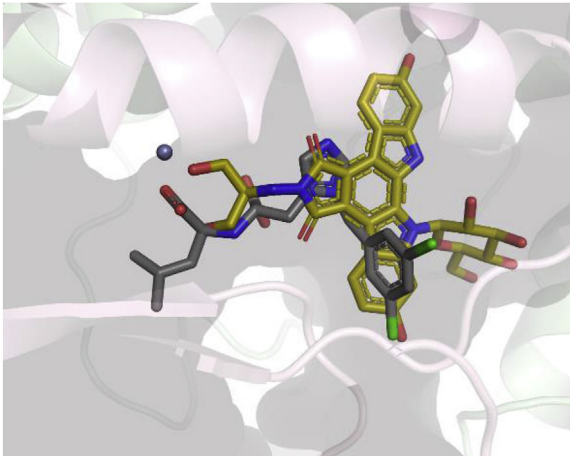
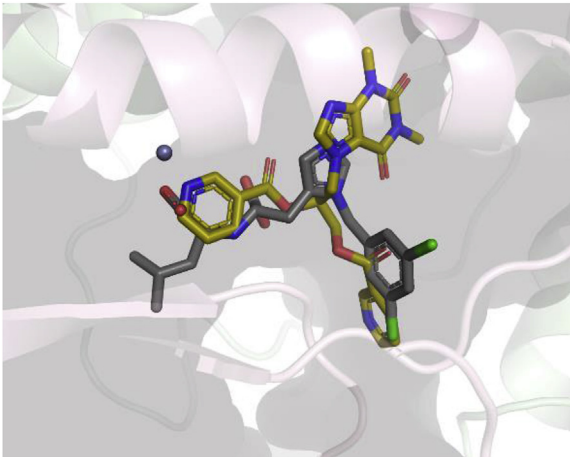
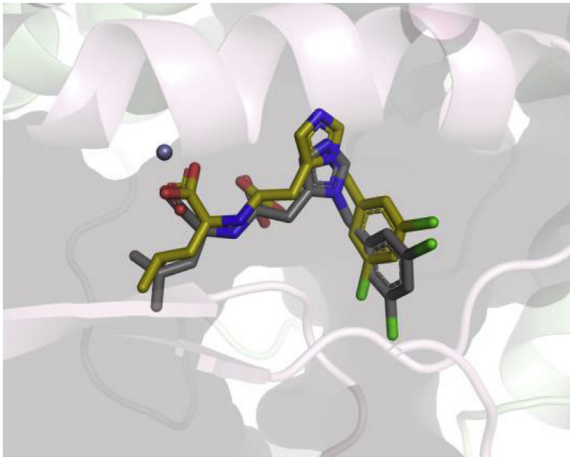
Drug	Binding energy (in kcal/mol)	Binding mode	Potential indications
<b>Fluprofylline</b> , a bronchodilator, anti-allergic and phosphodiesterase inhibitor	-1,785.00		Asthma and bronchitis; emphysema
<b>Pemetrexed</b> , a novel antimetabolite that inhibits folate-dependent enzymes such as thymidylate synthase	-1,602.58		Non-small cell lung cancer; pleural mesothelioma; other solid tumors
<b>Spirofylline</b> , a bronchodilator	-1,541.73		Asthma and bronchitis; emphysema

Table 1 (continued)

Drug	Binding energy (in kcal/mol)	Binding mode	Potential indications
<b>Edotecarin</b> , a potent DNA topoisomerase 1 inhibitor	-1,312.19		Esophageal and stomach cancer; breast cancer; glioblastoma; other solid tumors
<b>Diniprofylline</b> , a bronchodilator and phosphodiesterase inhibitor	-1,292.42		Asthma and bronchitis; emphysema
<b>MLN-4760</b> , the co-crystallized inhibitor	-309.93		Ulcerative colitis

been proposed for fighting the ongoing COVID-19 pandemic. Functionally, lividomycin acts as an aminoglycoside antibiotic, burixafor as a C-X-C chemokine receptor type 4 antagonist, quisnostat as a second generation histone deacetylase inhibitor, fluprofylline, spirofylline, and diniprofylline as phosphodiesterase inhibitors, pemetrexed as an antifolate, and edotecarin as a topoisomerase I inhibitor [39–43]. From this point of view, the

molecules display diverse structures with respect to functional group discrepancies reflecting their intended design as well as to pharmacophore variations. Indeed, favorable interactions calculated for each protein–ligand complex contribute to a better understanding of these molecule-based differences. There exists, however, a set of common interactions that occur between the drugs and the active-site residues of ACE2. The majority of these



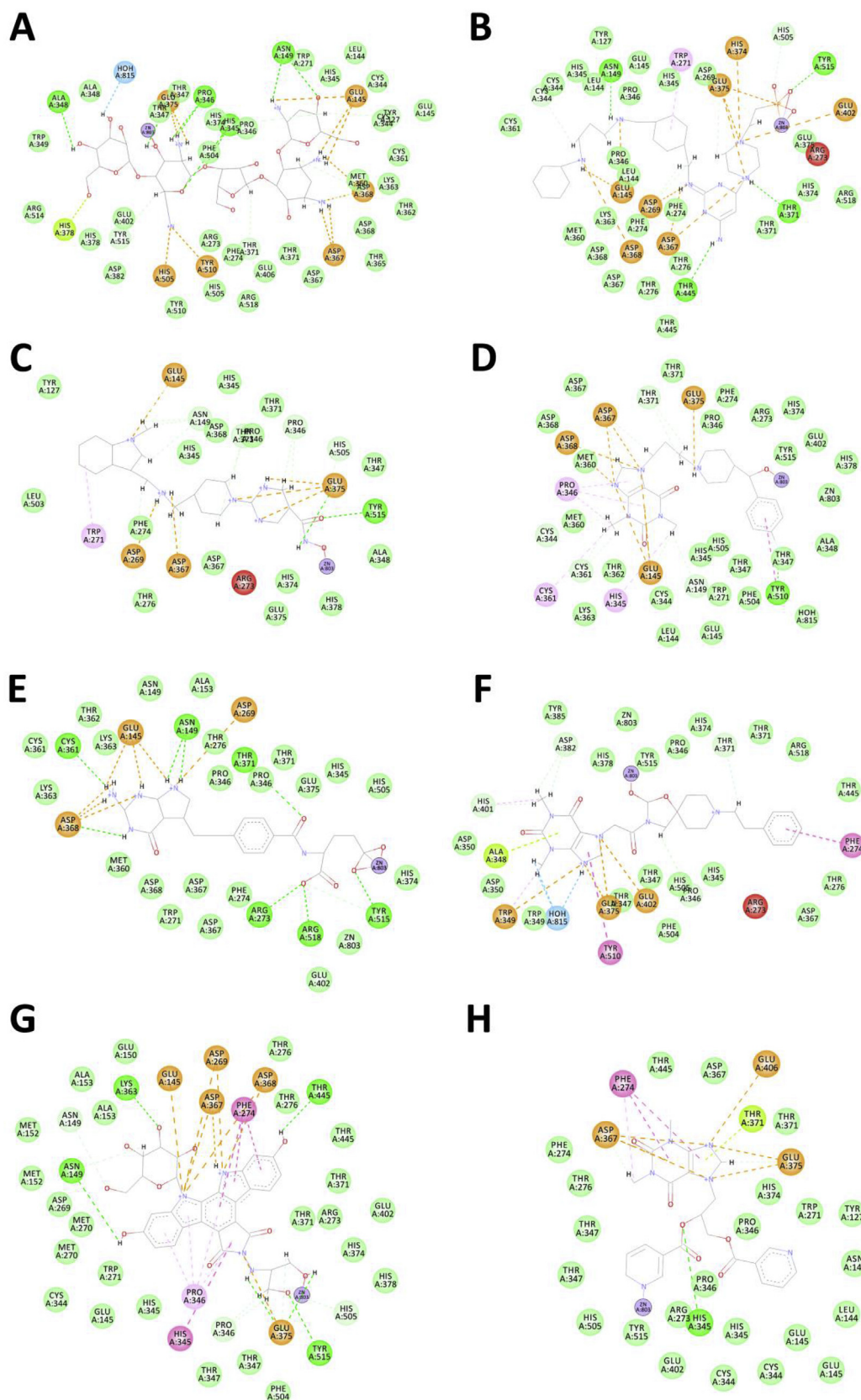


**Fig. 3.** Two-dimensional view of favorable interactions anchoring (A) lividomycin, (B) burixafor, (C) quisinostat, (D) fluprofylline, (E) pemetrexed, (F) spirofylline, (G) edotecarin, and (H) diniprofylline in the active-site cleft of human ACE2. Residues that are in van der Waals contact ( $< 4 \text{ \AA}$  distance) with ligand are shown as aqua green spheres. Ionic interactions (salt bridges), attractive charge interactions, and  $\pi$ -cation interactions are shown as orange dashed lines. Conventional hydrogen bonds are shown as lime green dashed lines. Weak hydrogen bonds are shown as light turquoise dashed lines.  $\pi$ - $\pi$  interactions (sandwich or T-shaped) are shown as magenta dashed lines.  $\pi$ -alkyl and alkyl-alkyl interactions are shown as pink dashed lines. The images were rendered using Discovery Studio Visualizer, Version 16.1.0 (Dassault Systèmes BIOVIA Corp., San Diego, CA, USA). (For interpretation of the references to color in this figure legend, the reader is referred to the Web version of this article.)

interactions are of the electrostatic type, and some are less prominent or even missing in the ACE2–MLN-4760 complex (Fig. 3). Firstly, in contrast to MLN-4760, the drugs bear more than one positive charge centers that increase their chances of establishing ion–ion interactions with the surrounding negatively charged side chains. Glu<sup>145</sup>, Asp<sup>269</sup>, Asp<sup>367</sup>, Asp<sup>368</sup>, and Glu<sup>375</sup> are among the most critical acidic residues in this regard since, in almost all cases, the drugs are attracted to at least two of these amino acids. Seven out of eight drugs (excluding pemetrexed) engage in ionic interactions with the catalytic residue Glu<sup>375</sup>, providing additional support for the potential inhibitory activities of the hits against ACE2. However, it is noteworthy to highlight that ionic interactions are also seen with other charged residues and that they are sometimes unique to the molecule in question. Secondly, each title molecule harbors a ZBG that is bound in a monodentate/bidentate fashion to the Zn<sup>2+</sup> ion cofactor, which is further ligated by the residues His<sup>374</sup>, His<sup>378</sup>, and Glu<sup>402</sup> respectively in a tetrahedral or square pyramidal coordination geometry. The phosphate group in burixafor, the carboxylate group in pemetrexed, the hydroxamate group in quisinostat, the pyridine ring in diniprofylline, the diol group in edotecarin, the alcohol group in lividomycin, and the ketone groups in fluprofylline and spirofylline are the core functionalities implemented within the potential binders. Thirdly, our inspections largely suggest structural variations in hydrogen-bonding interactions. Asn<sup>149</sup> and Tyr<sup>515</sup>, in particular, emerge as the key polar residues that secure the positions of many of the drugs within the active-site cleft of ACE2. Burixafor, quisinostat, pemetrexed, and edotecarin seem to be involved in hydrogen-bonding interactions with Tyr<sup>515</sup>, which is normally situated in sufficient proximity to the postulated tetrahedral intermediate for hydrogen bonding to occur during catalysis. Besides Asn<sup>149</sup> and Tyr<sup>515</sup>, several other residues from both subdomains are also important for firmly anchoring the drugs at the active site by side-chain and main-chain hydrogen bonds. Lastly, four drugs with conjugative  $\pi$ -planes (fluprofylline, spirofylline, edotecarin, and diniprofylline) are able to participate in  $\pi$ – $\pi$  interactions (sandwich or T-shaped) with the side chains of the surrounding residues Phe<sup>274</sup>, His<sup>345</sup>, and Tyr<sup>510</sup>. Trp<sup>271</sup> forms  $\pi$ –alkyl interactions with the hydrophobic portions of burixafor and quisinostat through its aromatic ring, while Pro<sup>346</sup> is involved in  $\pi$ –alkyl interactions with the conjugative  $\pi$ -planes of fluprofylline and edotecarin through its hydrophobic pyrrole moiety.

Intriguingly, it has been shown that proteolytic cleavage of ACE2 by TMPRSS2 is linked to increased uptake of SARS-CoV virions into permissive cells [44]. Therefore, it is likely that the drugs that were identified in this study interfere with TMPRSS2–ACE2 interactions, thereby further impeding viral entry (yet by a different route). However, it remains to be clearly demonstrated if the ligand-induced conformational change in the PD is transmitted to the rest of the extracellular portion of ACE2, and in particular toward the arginine-rich TMPRSS2 cleavage site (amino acid residues 697–716).

It is worth noting that in the presence of ACE2 inhibitors, acquired ACE2 deficiency is likely to occur in the long run. This may result in a shift in the balance between angiotensin II and angiotensin 1–7 in the favor of angiotensin II. An excess of angiotensin II activates local cardiac RAS, leading to heart failure [18]. Similarly, angiotensin II-induced activation of local pulmonary RAS has been linked to lung injury [45]. Therefore, additional protective measures may prove to be important in the clinical management of COVID-19. In order to compensate for the loss of ACE2 activity, soluble recombinant ACE2 PD and/or angiotensin 1–7 can be infused intravenously. Hypothetically speaking, soluble recombinant ACE2 PD does not only rescue some lost peptidase activity, but also facilitates the removal of SARS-CoV-2 from the circulation.

#### 4. Conclusion

Bearing in mind that ‘original’ drug development normally takes almost a decade of expensive research, drug repositioning is often hailed as a savior to countries affected by outbreaks. Here, we employed MM-assisted SBVS of a chemical library of several thousand clinically approved drugs and illustrated the key properties of the most promising repositionable drug candidates that possess the potential to interact with human ACE2 and prevent its recognition by SARS-CoV-2. The final shortlist of prospective viral-entry inhibitors (lividomycin, burixafor, quisinostat, fluprofylline, pemetrexed, spirofylline, edotecarin, and diniprofylline) awaits further validation in ACE2 activity assays as well as in membrane fusion assays. Besides the *in vitro* and *ex vivo* efficacy of the eight drugs mentioned above, several other parameters, such as their current status or stable presence in the drug market and their side-effect potential in case of testing of these drugs against SARS-CoV-2, should also be assessed by active clinicians in the relevant field. Nevertheless, given the urgency of fight against the current COVID-19 pandemic, it is now the appropriate time to introduce these and similar inhibitors going towards the clinics, either as stand-alone anti-COVID-19 drugs or in combination with other options including vaccines and M<sup>pro</sup>/RdRp inhibitors.

#### Data availability

All files are available from the corresponding author upon reasonable request.

#### Author contributions

KT: Conceptualization, Methodology, Formal analysis, Investigation, Writing. BB: Resources, Writing. HOG: Conceptualization, Formal analysis, Writing.

#### Declaration of competing interest

The authors declare that they have no known competing financial interests or personal relationships that could have appeared to influence the work reported in this paper.

#### Acknowledgements

This study was not supported financially by any grants.

#### References

- [1] WHO, Director-General's opening remarks at the media briefing on COVID-19—11 (n.d.), <https://www.who.int/dg/speeches/detail/who-director-general-s-opening-remarks-at-the-mediabriefing-%0Don-covid-19-11-march-2020>, March 2020.
- [2] World Health Organization, Coronavirus disease (COVID-19) situation report – 118 (n.d.), [https://www.who.int/docs/default-source/coronaviruse/situation-reports/20200517-covid-19-sitrep-118.pdf?sfvrsn=21c0d4fe\\_6](https://www.who.int/docs/default-source/coronaviruse/situation-reports/20200517-covid-19-sitrep-118.pdf?sfvrsn=21c0d4fe_6).
- [3] R. Lu, X. Zhao, J. Li, P. Niu, B. Yang, H. Wu, W. Wang, H. Song, B. Huang, N. Zhu, Y. Bi, X. Ma, F. Zhan, L. Wang, T. Hu, H. Zhou, Z. Hu, W. Zhou, L. Zhao, J. Chen, Y. Meng, J. Wang, Y. Lin, J. Yuan, Z. Xie, J. Ma, W.J. Liu, D. Wang, W. Xu, E.C. Holmes, G.F. Gao, G. Wu, W. Chen, W. Shi, W. Tan, Genomic characterisation and epidemiology of 2019 novel coronavirus: implications for virus origins and receptor binding, *Lancet* (2020), [https://doi.org/10.1016/S0140-6736\(20\)30251-8](https://doi.org/10.1016/S0140-6736(20)30251-8).
- [4] World Health Organization, “Solidarity” clinical trial for COVID-19 treatments, n.d. <https://www.who.int/emergencies/diseases/novel-coronavirus-2019/global-research-on-novel-coronavirus-2019-ncov/solidarity-clinical-trial-for-covid-19-treatments>.
- [5] P.A. Rota, M.S. Oberste, S.S. Monroe, W.A. Nix, R. Campagnoli, J.P. Icenogle, S. Peñaranda, B. Bankamp, K. Maher, M. hsin Chen, S. Tong, A. Tamin, L. Lowe, M. Frace, J.L. DeRisi, Q. Chen, D. Wang, D.D. Erdman, T.C.T. Peret, C. Burns, T.G. Ksiazek, P.E. Rollin, A. Sanchez, S. Liffick, B. Holloway, J. Limor, K. McCaustland, M. Olsen-Rasmussen, R. Fouchier, S. Günther, A.D.H.E. Osterhaus, C. Drosten,

- M.A. Pallansch, L.J. Anderson, W.J. Bellini, Characterization of a novel coronavirus associated with severe acute respiratory syndrome, *Science* (80-) (2003), <https://doi.org/10.1126/science.1085952>.
- [6] R.J.G. Hulswit, C.A.M. de Haan, B.J. Bosch, Coronavirus spike protein and tropism changes, in: *Adv. Virus Res.*, 2016, <https://doi.org/10.1016/bs.aivir.2016.08.004>.
- [7] M.A. Tortorici, D. Velesler, Structural insights into coronavirus entry, in: *Adv. Virus Res.*, 2019, <https://doi.org/10.1016/bs.aivir.2019.08.002>.
- [8] P. Zhou, X. Lou Yang, X.G. Wang, B. Hu, L. Zhang, W. Zhang, H.R. Si, Y. Zhu, B. Li, C.L. Huang, H.D. Chen, J. Chen, Y. Luo, H. Guo, R. Di Jiang, M.Q. Liu, Y. Chen, X.R. Shen, X. Wang, X.S. Zheng, K. Zhao, Q.J. Chen, F. Deng, L.L. Liu, B. Yan, F.X. Zhan, Y.Y. Wang, G.F. Xiao, Z.L. Shi, A pneumonia outbreak associated with a new coronavirus of probable bat origin, *Nature* (2020), <https://doi.org/10.1038/s41586-020-2012-7>.
- [9] M. Letko, A. Marzi, V. Munster, Functional assessment of cell entry and receptor usage for SARS-CoV-2 and other lineage B betacoronaviruses, *Nat. Microbiol.* (2020), <https://doi.org/10.1038/s41564-020-0688-y>.
- [10] K. Wang, W. Chen, Y.-S. Zhou, J.-Q. Lian, Z. Zhang, P. Du, L. Gong, Y. Zhang, H.-Y. Cui, J.-J. Geng, B. Wang, X.-X. Sun, C.-F. Wang, X. Yang, P. Lin, Y.-Q. Deng, D. Wei, X.-M. Yang, Y.-M. Zhu, K. Zhang, Z.-H. Zheng, J.-L. Miao, T. Guo, Y. Shi, J. Zhang, L. Fu, Q.-Y. Wang, H. Bian, P. Zhu, Z.-N. Chen, SARS-CoV-2 invades host cells via a novel route: CD147-spike protein, *BioRxiv* (2020), <https://doi.org/10.1101/2020.03.14.988345>.
- [11] W. Tai, L. He, X. Zhang, J. Pu, D. Voronin, S. Jiang, Y. Zhou, L. Du, Characterization of the receptor-binding domain (RBD) of 2019 novel coronavirus: implication for development of RBD protein as a viral attachment inhibitor and vaccine, *Cell. Mol. Immunol.* (2020), <https://doi.org/10.1038/s41423-020-0400-4>.
- [12] M. Hoffmann, H. Kleine-Weber, S. Schroeder, N. Krüger, T. Herrler, S. Erichsen, T.S. Schiergens, G. Herrler, N.H. Wu, A. Nitsche, M.A. Müller, C. Drosten, S. Pöhlmann, SARS-CoV-2 cell entry depends on ACE2 and TMPRSS2 and is blocked by a clinically proven protease inhibitor, *Cell* (2020), <https://doi.org/10.1016/j.cell.2020.02.052>.
- [13] A.C. Walls, Y.J. Park, M.A. Tortorici, A. Wall, A.T. McGuire, D. Velesler, Structure, function, and antigenicity of the SARS-CoV-2 spike glycoprotein, *Cell* (2020), <https://doi.org/10.1016/j.cell.2020.02.058>.
- [14] M. Donoghue, F. Hsieh, E. Baromas, K. Godbout, M. Gosselin, N. Stagliano, M. Donovan, B. Woolf, K. Robison, R. Jeyaseelan, R.E. Breitbart, S. Acton, A novel angiotensin-converting enzyme-related carboxypeptidase (ACE2) converts angiotensin I to angiotensin 1-9, *Circ. Res.* (2000), <https://doi.org/10.1161/01.res.87.5.e1>.
- [15] H. Zhang, Z. Kang, H. Gong, D. Xu, J. Wang, Z. Li, X. Cui, J. Xiao, T. Meng, W. Zhou, J. Liu, H. Xu, The digestive system is a potential route of 2019-nCoV infection: a bioinformatics analysis based on single-cell transcriptomes, *BioRxiv* (2020), <https://doi.org/10.1101/2020.01.30.927806>.
- [16] Y. Zhao, Z. Zhao, Y. Wang, Y. Zhou, Y. Ma, W. Zuo, Single-cell RNA expression profiling of ACE2, the putative receptor of Wuhan 2019-nCoV, *BioRxiv* (2020), <https://doi.org/10.1101/2020.01.26.919985>.
- [17] H. Zhang, J. Wada, K. Hida, Y. Tsuchiyama, K. Hiragushi, K. Shikata, H. Wang, S. Lin, Y.S. Kanwar, H. Makino, Collectrin, a collecting duct-specific transmembrane glycoprotein, is a novel homolog of ACE2 and is developmentally regulated in embryonic kidneys, *J. Biol. Chem.* (2001), <https://doi.org/10.1074/jbc.M006723200>.
- [18] M. Paul, A.P. Mehr, R. Kreutz, Physiology of local renin-angiotensin systems, *Physiol. Rev.* (2006), <https://doi.org/10.1152/physrev.00036.2005>.
- [19] D. Wrapp, N. Wang, K.S. Corbett, J.A. Goldsmith, C.L. Hsieh, O. Abiona, B.S. Graham, J.S. McLellan, Cryo-EM structure of the 2019-nCoV spike in the prefusion conformation, *Science* (80-) (2020), <https://doi.org/10.1126/science.aax0902>.
- [20] R. Yan, Y. Zhang, Y. Li, L. Xia, Y. Guo, Q. Zhou, Structural basis for the recognition of SARS-CoV-2 by full-length human ACE2, *Science* (80-) (2020), <https://doi.org/10.1126/science.abb2762>.
- [21] J. Lan, J. Ge, J. Yu, S. Shan, H. Zhou, S. Fan, Q. Zhang, X. Shi, Q. Wang, L. Zhang, X. Wang, Structure of the SARS-CoV-2 spike receptor-binding domain bound to the ACE2 receptor, *Nature* (2020), <https://doi.org/10.1038/s41586-020-2180-5>.
- [22] S.F. Ahmed, A.A. Quadeer, M.R. McKay, Preliminary identification of potential vaccine targets for the COVID-19 coronavirus (SARS-CoV-2) based on SARS-CoV immunological studies, *Viruses* (2020), <https://doi.org/10.3390/v12030254>.
- [23] G. Li, E. De Clercq, Therapeutic options for the 2019 novel coronavirus (2019-nCoV), *Nat. Rev. Drug Discov.* (2020), <https://doi.org/10.1038/d41573-020-00016-0>.
- [24] P. Towler, B. Staker, S.G. Prasad, S. Menon, J. Tang, T. Parsons, D. Ryan, M. Fisher, D. Williams, N.A. Dales, M.A. Patane, M.W. Pantoliano, ACE2 X-ray structures reveal a large hinge-bending motion important for inhibitor binding and catalysis, *J. Biol. Chem.* (2004), <https://doi.org/10.1074/jbc.M311191200>.
- [25] M.J. Huentelman, J. Zubcevic, J.A. Hernández Prada, X. Xiao, D.S. Dimitrov, M.K. Raizada, D.A. Ostrov, Structure-based discovery of a novel angiotensin-converting enzyme 2 inhibitor, *Hypertension* (2004), <https://doi.org/10.1161/01.HYP.0000146120.29648.36>.
- [26] J. Dyall, C.M. Coleman, B.J. Hart, T. Venkataraman, M.R. Holbrook, J. Kindrachuk, R.F. Johnson, G.G. Olinger, P.B. Jahrling, M. Laidlaw, L.M. Johansen, C.M. Lear-Rooney, P.J. Glass, L.E. Hensley, M.B. Frieman, Repurposing of clinically developed drugs for treatment of Middle East respiratory syndrome coronavirus infection, *Antimicrob. Agents Chemother.* (2014), <https://doi.org/10.1128/AAC.03036-14>.
- [27] H.M. Berman, J. Westbrook, Z. Feng, G. Gilliland, T.N. Bhat, H. Weissig, I.N. Shindyalov, The protein Data Bank, *Nucleic Acids Res.* (2000), <https://doi.org/10.1093/nar/28.1.235>. [www.rcsb.org](http://www.rcsb.org).
- [28] E.F. Pettersen, T.D. Goddard, C.C. Huang, G.S. Couch, D.M. Greenblatt, E.C. Meng, T.E. Ferrin, UCSF Chimera - a visualization system for exploratory research and analysis, *J. Comput. Chem.* (2004), <https://doi.org/10.1002/jcc.20084>.
- [29] N. Lagarde, E. Goldwaser, T. Pencheva, D. Jereva, I. Pajeva, J. Rey, P. Tuffery, B.O. Villoutreix, M.A. Miteva, A free web-based protocol to assist structure-based virtual screening experiments, *Int. J. Mol. Sci.* (2019), <https://doi.org/10.3390/ijms20184648>.
- [30] C.M. Labbé, J. Rey, D. Lagorce, M. Vavruša, J. Becot, O. Sperandio, B.O. Villoutreix, P. Tuffery, M.A. Miteva, MTiOpenScreen: a web server for structure-based virtual screening, *Nucleic Acids Res.* (2015), <https://doi.org/10.1093/nar/gkv306>.
- [31] C.M. Labbe, T. Pencheva, D. Jereva, D. Desvillechabrol, J. Becot, B.O. Villoutreix, I. Pajeva, M.A. Miteva, AMMOS2: a web server for protein-ligand-water complexes refinement via molecular mechanics, *Nucleic Acids Res.* (2017), <https://doi.org/10.1093/nar/gkx397>.
- [32] S. Salentin, S. Schreiber, V.J. Haupt, M.F. Adamsme, M. Schroeder, PLIP: fully automated protein-ligand interaction profiler, *Nucleic Acids Research* 43 (W1) (2015) W443–W447, <https://doi.org/10.1093/nar/gkv315>.
- [33] T. Pencheva, D. Lagorce, I. Pajeva, B.O. Villoutreix, M.A. Miteva, AMMOS: automated molecular mechanics optimization tool for in silico screening, *BMC Bioinf.* (2008), <https://doi.org/10.1186/1471-2105-9-438>.
- [34] S.R. Tipnis, N.M. Hooper, R. Hyde, E. Karran, G. Christie, A.J. Turner, A human homolog of angiotensin-converting enzyme: cloning and functional expression as a captopril-insensitive carboxypeptidase, *J. Biol. Chem.* (2000), <https://doi.org/10.1074/jbc.M002615200>.
- [35] G.I. Rice, D.A. Thomas, P.J. Grant, A.J. Turner, N.M. Hooper, Evaluation of angiotensin-converting enzyme (ACE), its homologue ACE2 and neprilysin in angiotensin peptide metabolism, *Biochem. J.* (2004), <https://doi.org/10.1042/BJ20040634>.
- [36] V. Putignano, A. Rosato, L. Banci, C. Andreini, MetalPDB in 2018: a database of metal sites in biological macromolecular structures, *Nucleic Acids Res.* (2018), <https://doi.org/10.1093/nar/gkx989>.
- [37] K. Kawai, N. Nagata, Metal-ligand interactions: an analysis of zinc binding groups using the Protein Data Bank, *Eur. J. Med. Chem.* (2012), <https://doi.org/10.1016/j.ejmech.2012.02.028>.
- [38] J.L. Guy, R.M. Jackson, H.A. Jensen, N.M. Hooper, A.J. Turner, Identification of critical active-site residues in angiotensin-converting enzyme-2 (ACE2) by site-directed mutagenesis, *FEBS J.* (2005), <https://doi.org/10.1111/j.1742-4658.2005.04756.x>.
- [39] L. Jin, Q. Guo, H.Y. Zhu, X.X. Xing, G.L. Zhang, M.F. Xuan, Q.R. Luo, Z.B. Luo, J.X. Wang, X.J. Yin, J.D. Kang, Quisinstat treatment improves histone acetylation and developmental competence of porcine somatic cell nuclear transfer embryos, *Mol. Reprod. Dev.* (2017), <https://doi.org/10.1002/mrd.22787>.
- [40] C. Korstanje, R. Sprenkels, H.N. Doods, J.G. Hugtenburg, E. Boddeke, H.D. Batink, M.J.M.C. Thoolen, P.A. Van Zwieten, Characterization of flupfylline, fluprofylline, ritanserine, butanserine and R 56413 with respect to in-vivo  $\alpha$ 1-,  $\alpha$ 2- and 5-HT2-receptor antagonism and in-vitro affinity for  $\alpha$ 1-,  $\alpha$ 2- and 5-HT2-receptors: comparison with ketanserine, *J. Pharm. Pharmacol.* (1986), <https://doi.org/10.1111/j.2042-7158.1986.tb04590.x>.
- [41] G. Fourcaud, F. Begassat, Expérimentation de la diniprofylline en gériatrie, *Therapeutique* 46 (3) (1970) 307–309.
- [42] K.D. Rollins, C. Lindley, Pemetrexed: a multitargeted antifolate, *Clin. Therapeut.* (2005), <https://doi.org/10.1016/j.clinthera.2005.09.010>.
- [43] M.W. Saif, R.B. Diasio, Edotecarin: a novel topoisomerase I inhibitor, *Clin. Colorectal Canc.* (2005), <https://doi.org/10.3816/CCC.2005.n.014>.
- [44] A. Heurich, H. Hofmann-Winkler, S. Gierer, T. Liepold, O. Jahn, S. Pohlmann, TMPRSS2 and ADAM17 cleave ACE2 differentially and only proteolysis by TMPRSS2 augments entry driven by the severe acute respiratory syndrome coronavirus spike protein, *J. Virol.* (2014), <https://doi.org/10.1128/jvi.02202-13>.
- [45] K. Kuba, Y. Imai, J.M. Penninger, Angiotensin-converting enzyme 2 in lung diseases, *Curr. Opin. Pharmacol.* (2006), <https://doi.org/10.1016/j.coph.2006.03.001>.